Novel chain structures in group VI elements

OLGA DEGTYAREVA[1]*, EUGENE GREGORYANZ[1], MADDURY SOMAYAZULU[2], PRZEMYSLAW DERA[1], HO-KWANG MAO[1] AND RUSSELL J. HEMLEY[1]

[1]Geophysical Laboratory, Carnegie Institution of Washington,5251 Broad Branch Road NW, Washington, District of Columbia 20015, USA
[2]HPCAT, Carnegie Institution of Washington, APS, 9700 South Cass Avenue, Argonne, Illinois 60439, USA
*e-mail: o.degtyareva@gl.ciw.edu

Published online: 23 January 2005; doi:10.1038/nmat1294

Recent developments in high-pressure methods and advances in X-ray crystallography have led to a new level of understanding of phase diagrams and structures of materials under pressure. Recently discovered phenomena such as complex phases of alkali metals[1,2], incommensurate host–guest structures[3,4], and incommensurately modulated structures[5,6] have rendered obsolete our conventional wisdom about the range of structures possible in the elements[7]. Using new *in situ* diffraction techniques, we have resolved the long-standing problem of the phase-transition sequence of sulphur in its non-metallic state. We demonstrate that it is very different from that previously proposed[7,8], with only two phases stable between 1.5 GPa and 83 GPa (the pressure of metallization), and temperatures from 300 K to 1,100 K. The phases have a triangular chain and a squared chain structure. The same squared chain structure is found in the heavier group VI element selenium.

Polymorphism of sulphur has been studied over the years by a wide range of techniques. Different experiments have produced conflicting results, mostly because all structural studies on lower-pressure phases have been performed only on quenched samples[9]. In fact, some 12 solid and 5 liquid phases have been reported, making the phase diagram of sulphur one of the most complicated among the elements[7]. Recent efforts with greatly improved experimental *in situ* high-pressure techniques, such as optical, spectroscopic or resistivity measurements, have revealed a wealth of interesting physical phenomena in sulphur, such as metallization at about 95 GPa (ref. 10), onset of superconductivity at 93 GPa with critical temperature T_c = 10 K (refs 11,12), increase of the superconducting transition temperature up to 17 K at around 160–200 GPa (refs 11,13), and existence of non-metallic and metallic liquids[14].

In situ high-pressure diffraction studies on the metallic phase of sulphur report a base-centred orthorhombic (b.c.o.) structure above 83 GPa (refs 15,16), which transforms at 162 GPa to a β-Po structure[16]. These metallic phases of sulphur are isostructural with the high-pressure metallic phases of the heavier group-VI elements selenium and tellurium[17–19]. The crystal structure of sulphur in the intermediate pressure range below metallization is unclear. Some *in situ* diffraction experiments[8] indicated a pressure-induced amorphization at 25 GPa, but the energy-dispersive X-ray diffraction technique used in that study can be misleading if large crystallites with preferred orientation form. Indeed, a phase with large crystallites has been reported above 25 GPa in an angle-dispersive X-ray diffraction study on sulphur but without structural determination[15].

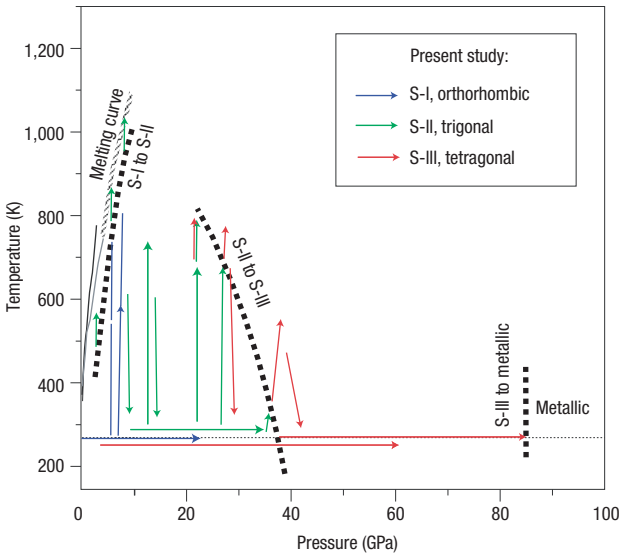

Figure 1 Reaction and transformation diagram of sulphur. Selected *P–T* paths of this study are shown with arrows, where the direction of the arrows indicate the increase/decrease of pressure/temperature. Blue arrows indicate the S-I phase, green arrows the S-II and red arrows the S-III phase. Melting curve up to 3 GPa, shown by the black solid line, is taken from ref. 9, melting curve up to 5 GPa, shown by grey solid line, is taken from ref. 21 and melting curve from 5 GPa to higher pressures, shown by dashed area, is taken from ref. 14. The boundaries for the transitions S-I to S-II and S-II to S-III observed in the present study are shown by dashed lines.

The most recent *in situ* study on the low-pressure phase diagram of sulphur[20,21] provided the first high-quality diffraction data on high-pressure sulphur. This study showed a transformation of the ambient-pressure S_8 ring molecule of the orthorhombic *Fddd* phase

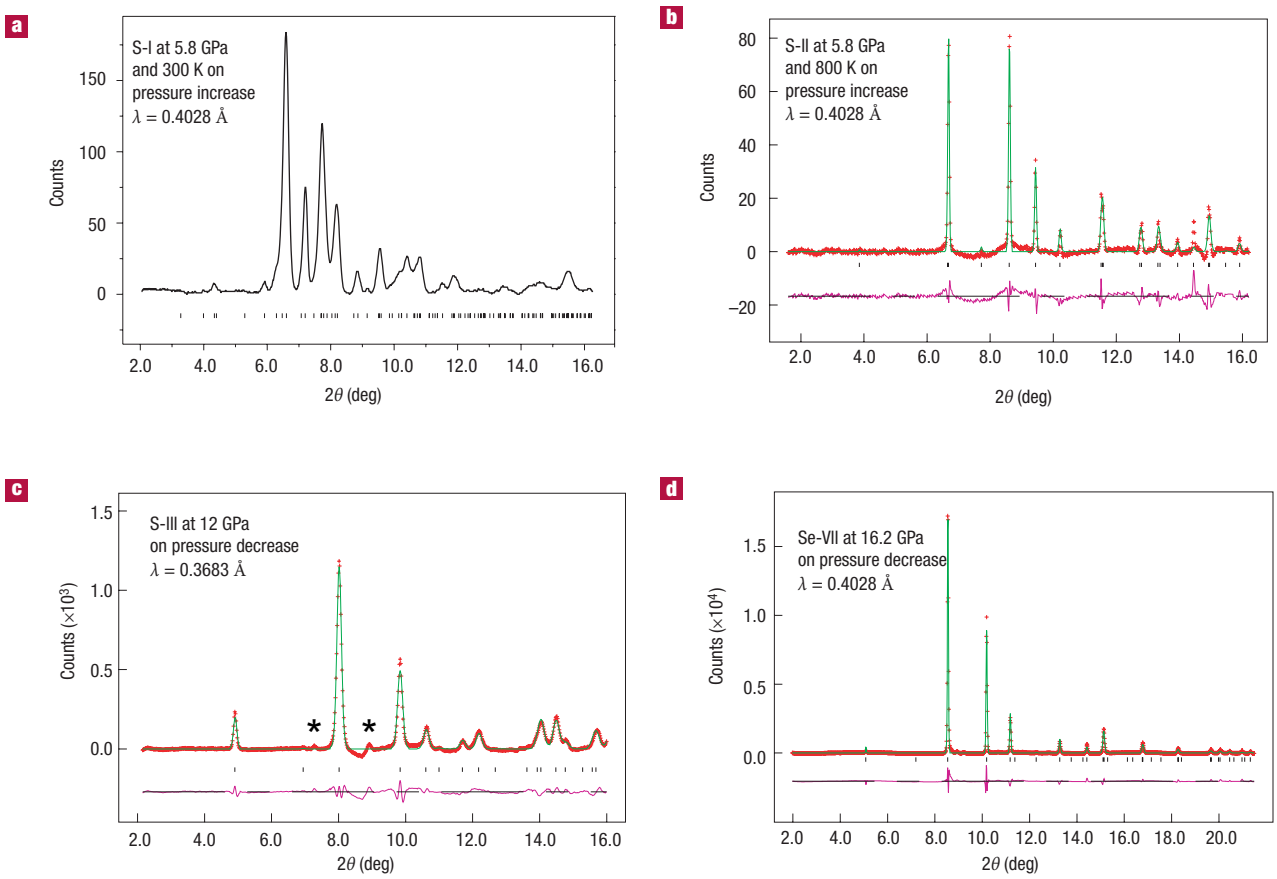

Figure 2 ***In situ*** **X-ray diffraction data**. X-ray spectra of **a**, S-I at 5.8 GPa and 300 K collected on pressure increase; **b**, S-II at 5.8 GPa and 800 K collected on pressure increase; **c**, S-III taken on pressure decrease at 12 GPa and 300 K; and **d**, Se-VII, taken on pressure decrease at 16 GPa and 300 K after heating to 450 K at 20 GPa. The spectra of S-I, S-II and Se-VII are taken with $\lambda = 0.4028$ Å; the spectrum of S-III is taken with $\lambda = 0.3683$ Å. Full structure Rietveld refinement is shown for the S-II, S-III and Se-VII phases. Red crosses, green solid lines and purple lines represent experimental, modelled and difference spectra. The ticks below profiles indicate the predicted peak positions. Asterisks in the S-III profile indicate the reflections from the pressure-transmitting medium N_2.

S-I to a new phase S-II, consisting of chains with trigonal geometry. Phase S-II is reported to form only on heating of S-I (because of a kinetic barrier) at pressures above 1.5 GPa. This study[20,21], however, was restricted to pressures of 5 GPa, leaving the behaviour of S-II in the pressure range between 5 and 83 GPa unknown. To understand the high-pressure behaviour of sulphur, we have conducted several angle-dispersive X-ray diffraction experiments using diamond anvil cells and monochromatic high-energy high-brilliance synchrotron radiation over a broad pressure–temperature (P–T) range.

Samples of S (99.999% purity, Puratronic) were loaded in high-temperature Mao-Bell cells with different openings allowing probing up to 22 degrees of 2θ. Different pressure-transmitting media (that is, He, Ne, N_2 and no medium) were used for different loadings. To determine the pressure, we used *in situ* fluorescence measurements of ruby chips loaded in the sample chamber. In the case of heating experiments, pressure was measured before and after heating and did not change appreciably. The temperatures were measured to within ±5 K by thermocouple. The high-temperature technique is described in greater detail in ref. 22 and references therein. Powder diffraction data were collected at beamline 16-ID-B (HPCAT) at the Advanced Photon Source. Focused, monochromatic beams of different wavelengths ($\lambda = 0.36 - 0.42$ Å) were used and the data were recorded on a MAR CCD (charge-coupled device) or image plate calibrated with a CeO_2 or silicon standard. Diffraction data were integrated azimuthally using FIT2D[23], and structural information was obtained by Rietveld refinement of the integrated profiles using GSAS[24].

Figure 1 shows the thermodynamic paths followed during this study. In all the runs, our diffraction data show that the starting material was always the known ambient S-I phase. On heating at pressures above 3 GPa, S-I transforms to S-II at temperatures very close to the melting line of sulphur (Fig. 1). The phase transition from S-I to S-II is of first order, and is associated with marked changes in the diffraction pattern (Fig. 2). The diffraction patterns of phase S-II were indexed with trigonal unit cell ($a = 6.9082(3)$ Å, $c = 4.2593(6)$ Å, atomic volume $V = 19.54$ Å^3 at 5.8 GPa and 800 K). Rietveld refinement confirmed that the S-II phase forms the trigonal structure with space group $P3_221$, reported in ref. 20, that consists of triangular chains, running parallel to the trigonal c-axis, with three atoms per turn (Fig. 3). Our Rietveld refinement (Fig. 2) showed that the atoms occupy the following positions: 3(b) (0.876(4) 0 1/6) and 6(c) (0.230(3) 0.534(2) 0.051(3)), close to those reported previously[20], and yielded R-factors R_{wp} =7.6%, R_p = 5.4%.

The S-II phase closely resembles ambient polymorphs of the heavier group VI elements selenium and tellurium[7], consisting of atomic chains with similar geometry (Fig. 3). The bond angle and the torsion angle in S-II are very similar to those in Se-I and Te-I. But the structure of S-II with two symmetry-independent spirals per

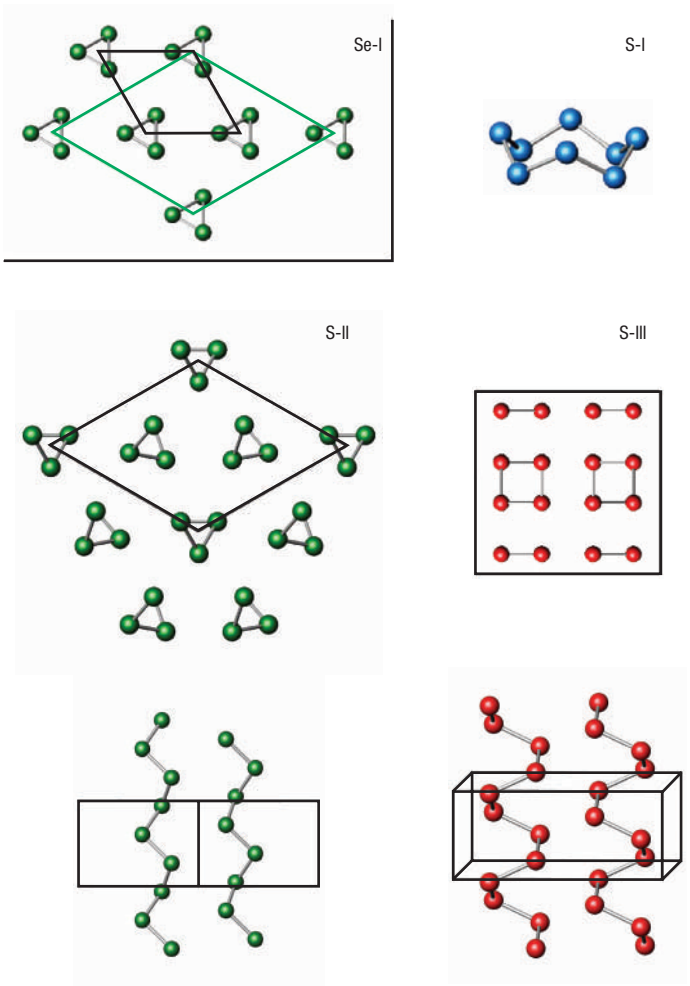

Figure 3 Crystal structures of Se and S. Structure of Se-I with black line indicating Se-I cell and green line indicating S-II cell; S_8 ring molecule of S-I; trigonal chain structure of S-II and tetragonal chain structure of S-III. The bonds up to 2.10 Å for S and 2.32 Å for Se are shown. The structures drawn for Se-I and S-I are based on the data from ref. 31.

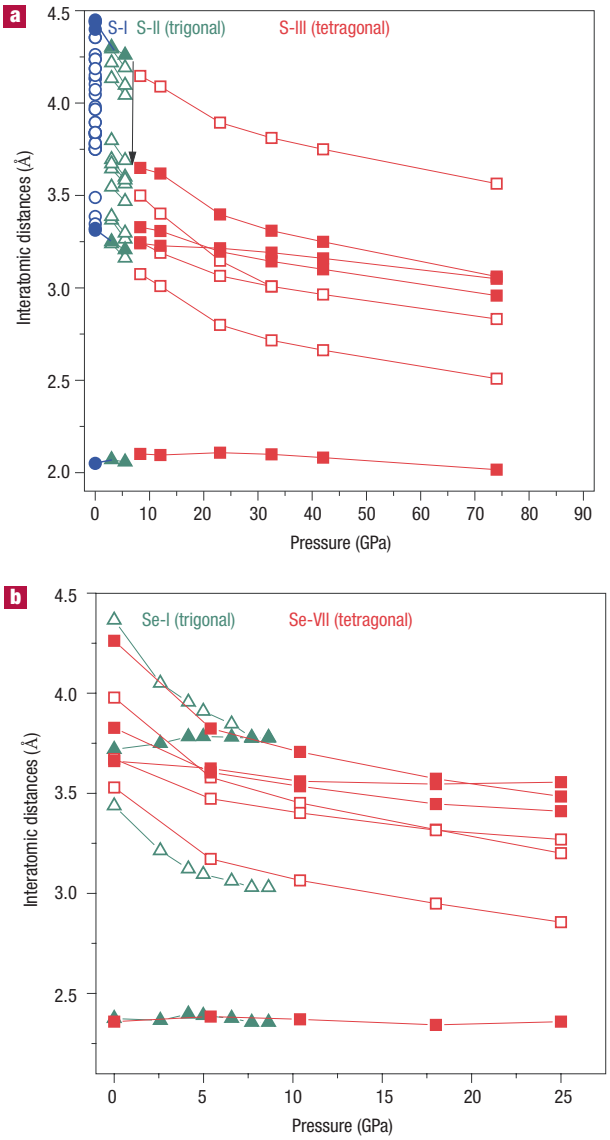

Figure 4 Pressure dependence of interatomic distances for S and Se. Data on S-II at 5.8 GPa, S-III and Se-VII are from present work. The interatomic bonds for S-I at atmospheric pressure and for S-II at 3.0 GPa are calculated using the data from refs 31 and 20, respectively. Data for Se-I are taken from ref. 25. Intrachain (intramolecular) interatomic distances are shown by solid symbols, whereas interchain (intermolecular) interatomic distances are shown by open symbols. The arrow shows the discontinuous change in *c*-lattice parameter (chain step) at the transition from S-II to S-III.

unit cell is more complex than the structure of Se-I and Te-I with one spiral per unit cell. In S-II, the spirals are rotated around the *c*-axis, if compared with those in Se-I (Fig. 3). The peculiar behaviour of the spiral chains in Se-I and Te-I in stretching under pressure, associated with an increasing *c* lattice parameter[19,25], is not observed in sulphur, where the *c* lattice parameter decreases slightly with pressure.

If sulphur is pressurized above 36 GPa at 300 K or heated at pressures between 22 and 35 GPa to temperatures shown in Fig. 1, it transforms into a body-centred-tetragonal phase S-III, quenchable in temperature down to 300 K (Fig. 2). The transformation also appears to be of first order. The S-III phase is stable up to 83 GPa at 300 K, where it transforms to the known metallic S-IV phase[15,16]. On pressure decrease at 300 K, S-III can be retained in a metastable form down to 3 GPa, where it transforms to another (metastable) phase with very broad diffraction peaks, the structure of which could not be determined. This phase transforms to S-I on decompression. Other (metastable) phases were observed on pressure decrease if sulphur was heated up to 850 K in the pressure range of 5–15 GPa (these phases are not discussed here). The patterns of S-III were indexed with the cell parameters $a = 8.5939(9)$ Å, $c = 3.6179(5)$ Å and $V = 16.70$ Å^3 at 12 GPa and 300 K on pressure decrease. The diffraction pattern of sulphur at 76.3 GPa reported previously[15] is likely to correspond to the S-III phase. The Rietveld refinement for S-III (Fig. 2) shows that the S atoms occupy 16(*f*) position (x x+1/4 1/8) of the space group $I4_1/acd$ (origin choice 2), with $x = 0.1405(3)$ at 12 GPa and 300 K (R-factors $R_{wp} = 5.1\%$, $R_p = 3.4\%$). The S-III structure consists of squared chains, running parallel to the tetragonal *c*-axis, with four atoms per turn (Fig. 3). This is a novel structure type. Similar chains of S atoms have been reported[26] for a high-pressure phase of H_2S, but the closest S–S distance in this structure (3.05 Å at 14 GPa) is much larger than 2.10 Å in S-III.

We have reproduced the S-I to S-II transition several times at different pressures and temperatures (Fig. 1). The S-II phase always forms just below the melting line and after re-crystallization from the liquid state, and is quenchable in temperature down to 300 K. This phase is stable at 300 K up to 36 GPa, and has a negative slope of transformation to S-III, similar to that observed[27] in molecular phases of N_2. The experiments carried out at high pressures, loading sulphur in different pressure-transmitting media and following different P–T paths by heating S-I or S-II at different pressures, all resulted in the formation of S-III above 36 GPa at room temperature.

We carried out diffraction experiments on the next member of the chalcogen family, Se, taking its trigonal polymorph as a starting material. It is found to transform at elevated pressures and temperatures to a tetragonal phase of squared chains, identical to S-III, called here Se-VII. At 16.2 GPa, Se-VII has unit cell parameters of $a = 9.0753(1)$ Å, $c = 3.6206(1)$ Å and $V = 18.63$ Å^3 (Fig. 2). Rietveld refinement gives the atomic position parameter $x = 0.1293(2)$ (R-factors $R_{wp} = 2.4\%$ and $R_p = 1.3\%$). Unlike S, Se-VII can be reached only by heating (for example, 450 K at 20 GPa), and can be quenched to ambient temperature and pressure. If further pressurized at room temperature, Se-VII transforms at 29 GPa to the known metallic Se-IV phase[5,18]. Diffraction patterns similar to Se-VII have been observed in recent high-pressure studies[28] of orthorhombic Se in the pressure range 12–23 GPa. The diffraction data for S-II, S-III and Se-VII measured as a function of pressure provide a direct determination of the equation of state (see Supplementary information Fig. S1).

Our results demonstrate that the S_8 molecular rings of S-I break under pressure and form triangular chains of S-II, which at higher pressure rearrange into squared chains of S-III with a tighter spiral pitch and denser structure. Through the pressure-induced conformational transformation of atomic chains from trigonal to tetragonal geometry, the shortest covalent S–S (Se–Se) interatomic distance of ~2.10 Å (~2.32 Å) and the next-nearest intrachain distance remain essentially invariant (Fig. 4). The change in bond angle through the phase transitions is not large (100–108°). However, the torsion angle is much smaller in S-III (46.7° at 12 GPa) than the 98.7° in S-I at ambient pressure and 97.5° in S-II at 5.8 GPa.

Our findings show parallels with the ground-state structures and energy landscapes predicted in density functional calculations for isolated molecules and clusters (ref. 29 and references therein; ref. 30). Specifically, the calculations predict the stability of both rings and chains with nearly constant S–S bond lengths together with comparable bond angles and conformational freedom about torsion angles. Comparison between theory and experiment indicates that the structures in S and Se are controlled to first order by localized bonding properties over a broad range of compression (that is, up to metallization).

Received 4 March 2004; accepted 5 November 2004; published 23 January 2005.

References

1. Hanfland M., Syassen, K. Christensen, N. E. & Novikov D. L. New high-pressure phases of lithium, *Nature* **408,** 174–178 (2000).
2. Nelmes, R. J., McMahon, M. I., Loveday, J. S. & Rekhi, S. Structure of Rb-III: novel modulated stacking structures in alkali metals. *Phys. Rev. Lett.* **88,** 155503 (2002).
3. Nelmes, R. J., Allan, D. R., McMahon, M. I. & Belmonte, S. A. Self-hosting incommensurate structure of barium IV. *Phys. Rev. Lett.* **83,** 4081–4084 (1999).
4. McMahon, M. I., Degtyareva, O. & Nelmes, R. J. Ba-IV-type incommensurate crystal structure in group-V metals. *Phys. Rev. Lett.* **85,** 4896–4899 (2000).
5. Hejny, C. & McMahon, M. I. Large structural modulations in incommensurate Te-III and Se-IV, *Phys. Rev. Lett.* **91,** 215502 (2003).
6. Takemura, K., Sato, K., Fujihisa, H. & Onoda, M. Modulated structure of solid iodine during its molecular dissociation under high pressure. *Nature* **423,** 971–974 (2003).
7. Young, D. A. *Phase Diagrams of the Elements* (Univ. California Press, Oxford, UK, 1991).
8. Luo, H. & Ruoff, A. L. X-ray diffraction study of sulfur to 32 GPa: amorphization at 25 GPa. *Phys. Rev. B* **48,** 569–572 (1993).
9. Vezzoli, G. C., Dachille, F. & Roy, R. Sulfur melting and polymorphism under pressure: outlines of fields for 12 crystalline phases. *Science* **166,** 218–221 (1969).
10. Luo, H., Desgreniers, S., Vohra, Y. & Ruoff, A. L. High-pressure optical studies on sulfur to 121 GPa: Optical evidence for metallization. *Phys. Rev. Lett.* **67,** 2998–3001 (1991).
11. Struzhkin V. V., Hemley, R. J., Mao, H. K. & Timofeev, Yu.A. Superconductivity at 10–17 K in compressed sulphur. *Nature*, **390,** 382–384 (1997).
12. Kometani, S., Eremets, M. I., Shimizu, K. Kobayashi, M. & Amaya, K. Observation of pressure-induced superconductivity of sulphur. *J. Phys. Soc. Jpn* **66,** 2564–2565 (1997).
13. Gregoryanz, E. *et al.* Superconductivity in the chalcogens up to multimegabar pressures. *Phys. Rev. B* **65,** 064504 (2002).
14. Brazhkin, V. V., Popova, S. V. & Voloshin, R. N. Pressure-temperature phase diagram of molten elements: selenium, sulfur and iodine. *Physica B* **265,** 64–71 (1999).
15. Akahama, Y., Kobayashi, M. & Kawamura, H. Pressure-induced structural phase transition in sulfur at 83 GPa. *Phys. Rev. B* **48,** 6862–6864 (1993).
16. Luo, H., Greene, R. G. & Ruoff, A. L. β-Po phase of sulfur at 162 GPa: X-ray diffraction study to 212 GPa. *Phys. Rev. Lett.* **71,** 2943–2946 (1993).
17. Aoki, K., Shimomura, O. & Minomura, S. Crystal structure of the high-pressure phase of tellurium. *J. Phys. Soc. Jpn* **48,** 551–556 (1980).
18. Akahama, Y., Kobayashi, M. & Kawamura, H. Structural studies of pressure-induced phase transitions in selenium up to 150 GPa. *Phys. Rev. B* **47,** 20–26 (1993).
19. Jamieson J. C. & McWhan, D. B. Crystal structure of tellurium at high pressure. *J. Chem. Phys.* **43,** 1149 (1965).
20. Crichton, W. A., Vaughan, G. B. M. & Mezouar, M. *In situ* structure solution of helical sulphur at 3 GPa and 400 °C. *Z. Kristallogr.* **216,** 417–419 (2001).
21. Mezouar, M. Program, School on Crystallography at High Pressure, Erice, 2003. http://erice2003.docking.org/Mezouar2.ppt
22. Gregoryanz, E., Goncharov, A. F., Matsuishi, K., Mao H.-K. & Hemley, R. J. Raman spectroscopy of hot dense hydrogen. *Phys. Rev. Lett.* **90,** 175701 (2003).
23. Hammersley, A. P., Svensson, S. O., Hanfland, M., Fitch, A. N. & Hausermann, D. Two-dimensional detector software: from real detector to idealised image or two-theta scan. *High Press. Res.* **14,** 235–248 (1996).
24. Larson A. C. & Von Dreele, R. B. *GSAS Manual.* Rep. LAUR 86–748 (Los Alamos Natl Lab., Los Alamos, 1988).
25. Keller, R. Holzapfel, W. B. & Schulz, H. Effect of pressure on the atom positions in Se and Te. *Phys. Rev. B* **16,** 4404–4412 (1977).
26. H. Fujihisa, H. *et al.* Structures of H_2S: phases I and IV under high pressure. *Phys. Rev. B* **57,** 2651–2654 (1998).
27. Gregoryanz, E. *et al.* Raman, infrared, and X-ray evidence for new phases of nitrogen at high pressures and temperatures. *Phys. Rev. B* **66,** 224108 (2002).
28. Nakano, K., Akahama, Y., Kawamura, H., Takumi, M. & Nagata, K. Pressure-induced metallization and structural transition of orthorhombic Se. *Phys. Status Solidi B* **223,** 397–400 (2001).
29. Hohl, D., Jones, R. O., Car, R. & Parrinello, M. Structure of sulfur clusters using simulated annealing: S_2 to S_{13}. *J. Chem. Phys.* **89,** 6823–6835 (1988).
30. Jones, R. O. & Ballone, P. Density functional and Monte Carlo studies of sulfur. I. Structure and bonding in S_n rings and chains ($n = 2$–18). *J. Chem. Phys.* **118,** 9257–9265 (2003).
31. Donohue, J. *The Structures of the Elements* (Krieger, Florida, 1982).

Acknowledgements

We thank V. F. Degtyareva for helpful discussions. This work and HPCAT is supported by DOE-BES, DOE-NNSA, DOD-TACOM, NSF, NASA and the W.M. Keck Foundation. The authors acknowledge financial support from NSF, through grant EAR-0217389. The Advanced Photon Source is supported by the US Department of Energy, Office of Science, Office of Basic Energy Sciences, under Contract No. W-31-109-Eng-38.

Correspondence and requests for materials should be addressed to O.D.

Supplementary Information accompanies the paper on www.nature.com/naturematerials.

Competing financial interests

The authors declare that they have no competing financial interests.

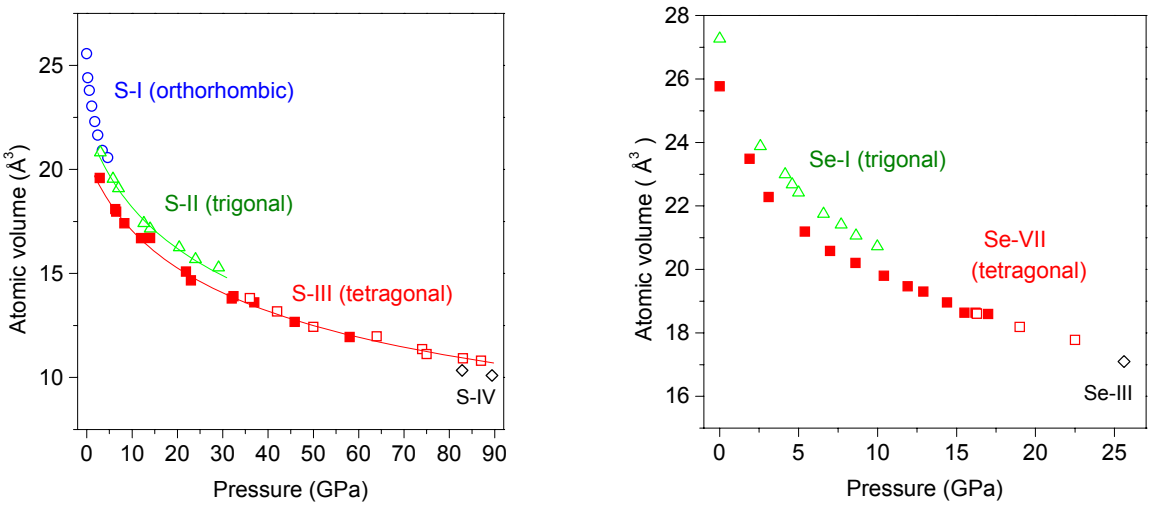

Supplementary Figure 1. **Equations of state for S and Se.** Data on S-I (blue circles), S-II (green triangles), S-III and Se-VII (red squares) are from present work. Data for Se-I (green triangles) are taken from Ref. [1]; data for S-IV and Se-III are taken from Ref [2] and [3], respectively. The data collected on pressure increase are shown with open symbols, data collected on pressure decrease are shown with solid symbols. The fitting of the pressure-volume data with the second-order Birch-Murnaghan equation of state (shown by solid lines) gives for S-II Ko= 34(2)GPa, V/Vo=0.867(1), and for S-III Ko=37(1)GPa, V/Vo=0.804(1), with Vo=25.56Å and Ko' = 4 for both phases. The volume difference between the S-II and S-III phases is 6.5% at 6.2 GPa, and between the Se-I and Se-VII phases, it is 5.6% at ambient pressure.

[1] R. Keller, W.B. Holzapfel, and H. Schulz, Effect of pressure on the atom positions in Se and Te, *Phys. Rev. B* **16**, 4404 (1977).
[2] Y. Akahama, M. Kobayashi, H. Kawamura, Pressure-induced structural phase transition in sulfur at 83 GPa, *Phys. Rev. B* **48**, 6862 (1993).
[3] C. Hejny and M.I. McMahon, Complex crystal structures of Te-II and Se-III at high pressure, *Phys. Rev. B* **70**, 184109 (2004).